Biointerface Research in Applied Chemistry

Protective potentials of a siderophore receptor against *Acinetobacter baumannii* infections

Zahra Aghajani [1], Iraj Rasooli [1, 2, *], Seyed Latif Mousavi Gargari [1]

[1]Department of Biology, Shahed University, Tehran, Iran
[2]Molecular Microbiology Research Center, Shahed University, Tehran, Iran

*corresponding author e-mail address: *rasooli@shahed.ac.ir*

ABSTRACT

Acinetobacter baumannii causes nosocomial infections and high mortality rates in the world. Since antibiotic treatment is complicated by extensive drug resistance in *A. baumannii* strains, other approaches such as vaccination can be a cost-effective solution. Siderophore receptor related to cluster 1 of iron uptake system (WP_000413999) is expressed in early stages of *A. baumannii*'s infection under iron restricted conditions. In this study, structural characterization and immunogenicity of the target protein in a murine sepsis model were assessed. Structural properties of the siderophore receptor were determined by bioinformatics tools. The gene encoding the antigen was cloned in *E. coli* BL21(DE3) and was then expressed. The purified recombinant protein was administered to the mice subcutaneously for antibody production. The immunized mice were challenged with the *A. baumannii* at lethal dose via intraperitoneal injection. Blast results revealed more than 97% identity of the protein in 3472 strains of *A. baumannii*. This receptor is a TonB-dependent transporter with a barrel domain composed of 22 β-strands connected by external loops and periplasmic turns. Experimental findings showed that the recombinant protein had no toxicity effect on A549 cells. Moreover, the studied protein was able to induce a specific antibody response in the mice. Survival rate of the passive immunized mice was improved against sepsis caused by *A. baumannii* ATCC 19606 and ABI022 clinical isolate. The study indicated that this siderophore receptor can be considered for further analysis as a potential vaccine target against *A. baumannii*.

Keywords: *Acinetobacter baumannii; Siderophore receptor; Antibody response; Passive immunization; Sepsis model.*

1. INTRODUCTION

Acinetobacter baumannii, an opportunistic pathogen, causes a wide range of nosocomial infections including pneumonia, bacteremia, infections of skin and soft tissue, catheter-associated urinary tract infections, meningitis and endocarditis [1]. Resistant to disinfectants, desiccation, and biofilm formation on the abiotic surfaces, make *A. baumannii* as a successful pathogen in hospital environments [2]. Due to emerging new pan-drug resistant (PDR) strains and high mortality rate of *A. baumannii* infections, World Health Organization (WHO) classified this pathogen in the priority I, a tier in which introducing new non-antibiotics treatments is strongly demanded [3]. Vaccination would be a proper solution to reduce the clinical and economic load of infections caused by *A. baumannii*. In this regard, various virulence factors of *A. baumannii* including capsular polysaccharide, biofilm associated protein (Bap), Acinetobacter trimeric autotransporter (Ata), OmpA, Omp22, OmpW, BauA, FilF, NucAb, BamA, SmpA, PLD as well as inactivated or attenuated whole cell, outer membrane complexes (OMCs) and outer membrane vesicles (OMVs) have been examined [4-18]. However, there is no safe and effective vaccine for human use. So, efforts are continued to identify new targets.

A. baumannii requires iron to perform different biological processes, while, it faces the iron-restricted environment in the host. Therefore, the cellular acquisition element of iron is considered a virulence factor [19, 20]. Several iron uptake systems have been described in *A. baumannii* among which the production of siderophores is the most important mechanism [21, 22]. Siderophores are low-molecular-weight molecules which chelate iron and enter the cells through outer membrane siderophore receptors. These receptors are crucial to full pathogenicity of *A. baumannii* [19].

It seems that antibody production develops a proper immunity to restrict *A. baumannii* infections [14, 15]. Therefore, as the accessibility of antigenic target to interact with antibodies is an important issue, outer membrane proteins (OMPs) are of interest as vaccine targets [23]. Siderophore receptor located in cluster I is a putative protein expressed in iron depletion condition [24], up-regulation of which was detected in pellicle form of *A. baumannii* [25] and *in vivo* in bacteremia animal model [26]. However, there is no data explaining its structure and immunogenicity analysis which can be helpful for better understanding this protein.

Objectives.

This study was aimed at characterization and determination of physico-chemical properties and 3D structure of WP_000413999. In order to validate the immunogenicity of selected protein *in vivo*, a murine sepsis model was set and the findings are discussed.

2. MATERIALS AND METHODS

Sequence availability.
The sequence of outer membrane siderophore receptor from cluster I in *A. baumannii* ATCC 19606 with GenPept accession number WP_000413999 from http://www.ncbi.nlm.nih.gov/protein served as the query for

BLAST against non-redundant protein (http://blast.ncbi.nlm.nih.gov/Blast.cgi).
Physicochemical characterization and subcellular localization.
Presence of signal peptidase I cleavage site was evaluated by, LIPOP (http://www.cbs.dtu.dk/services/LipoP/). In all other parts,

the mature protein without signal peptide was provided as a query for further analysis. The physicochemical properties of selected protein sequence such as theoretical isoelectric point (pI), molecular weight, amino acid composition, instability index, estimated half-life, aliphatic index, and grand average of hydropathicity (GRAVY) were analyzed using ProtParam tool (https://web.expasy.org/protparam/) [27].

β-barrel outer membrane protein predictor (BOMP) (http://www.bioinfo.no/tools/bomp) [28] and TMBETADISC-RBF (http://rbf.bioinfo.tw/~sachen/OMP.html) [29] were used for sequence analysis as to whether the protein belongs to an integral outer membrane protein. BOMP server identifies integral β-barrel proteins based on typical C-terminal pattern of many integral β-barrel proteins and scoring according to the presence of usual amino acids that participate in trans-membrane β-strands. The precision of predictions was >80%. TMBETADISC-RBF server discriminates OMPs by a method based on radial basis function (RBF) networks and the position specific scoring matrix (PSSM) profiles with an accuracy of 96.4%. Prediction of the subcellular localization was performed by CELLO2GO (http://cello.life.nctu.edu.tw/cello2go/) [30].

Secondary and tertiary structure prediction.
SEGMER (https://zhanglab.ccmb.med.umich.edu/SEGMER/) [31] was used to characterize the secondary structure of WP_000413999. In SEGMER, a threading algorithm is applied for recognizing substructure motifs.

PSI-BLAST at https://blast.ncbi.nlm.nih.gov/Blast.cgi, was used to identify homologues structures in Protein Data Bank (PDB). Tertiary structure was provided using I-TASSER (https://zhanglab.ccmb.med.umich.edu/I-TASSER/) [32], SPARKS-x (http://sparks-lab.org/yueyang/server/SPARKS-X/) [33], and ROBETTA (http://robetta.bakerlab.org/submit.jsp) [34] servers. I-TASSER and SPARKS-x utilize multiple threading alignments and fold recognition method for predicting the structure of a protein, respectively. ROBETTA approach is based on ab initio and comparative modeling. Quality of 3D predicted models were validated using Qmean (https://swissmodel.expasy.org/qmean/) [35] and Ramachandran plot (http://mordred.bioc.cam.ac.uk/~rapper/rampage.php). Qmean evaluates major geometrical aspects of protein structures by analyzing torsion angle potential over three consecutive amino acids, solvation potential, secondary structure specific distance-dependent pairwise residue-level potential, consensus predicted and calculated secondary structure, and solvent accessibility. This tool identifies the native structure and discriminates good from bad models. The final model was introduced after refinement by 3Drefine (http://sysbio.rnet.missouri.edu/3Drefine/) server which utilizes two-step protocol, including optimization of hydrogen bonding network and minimization of atomic level energy to improve qualities of the structures of the initial models to close it to native form [36]. Quality improvement of the refined model was assessed by Qmean and Ramachandran plot.

Position of the protein in the membrane.
PPM server (Positioning of Protein in Membrane) (http://opm.phar.umich.edu/server.php) was used for calculation of the spatial orientation of newly determined protein structures in membranes from PDB entries. Prediction of positioning is based on the evaluation of free energy of transfer of molecules from water to the lipid environment [37].

Bacterial strains and vector.
Acinetobacter baumannii ATCC 19606 was used for gene amplification and cloning. This standard strain and a clinical strain (ABI022, wound isolate) from the bacterial culture collection of Shahed University, were used for the establishment of murine sepsis. *Escherichia coli* BL21 (DE3) was used as an expression host for protein production. Bacterial strains were cultured in Luria-Bertani (LB) broth or agar at 37°C. For mice challenge, *A. baumannii* was grown under iron limited condition in LB supplemented with 2,2′-bipyridyl (200 μM). Kanamycin (70 μg/ml), was used in expression media as a selection marker.

PCR amplification.
The gene encoding WP_000413999 was amplified from *A. baumannii* ATCC 19606 chromosomal DNA using designed forward (5'-GCAGAATTCATGGAAACCGTAACTCAAACGGCTGAG-3') and reverse (5'-GCGCGCGGCCGCTTAATAGTTAAAAGTATAACTTAAACC-3') primers with *EcoRI* and *NotI* restriction sites, respectively. The polymerase chain reaction (PCR) amplification was performed with *pfu* DNA polymerase under the following condition: 94°C for 5 min, 35 cycles of 60 s at 94°C, 40 s at 65°C, and 2.5 min at 72°C, with a final extension at 72°C for 5 min. Colony PCR was also performed using clinical isolate as a template to check the presence of the studied gene.

Cloning and purification of recombinant proteins.
The purified product of the PCR and the vector (pET28a) were digested by restriction enzymes, followed by ligation with T4 DNA ligase. The ligation mixture was then transformed into *E. coli* BL21(DE3) competent cells by heat shock process. Transformants were selected on LB agar containing kanamycin and confirmed using PCR, enzymatic digestion, and sequencing.

For protein expression, LB broth containing antibiotic marker were inoculated by overnight grown culture of approved transformants. The cultures were induced by isopropyl β-D-1-thiogalactoside (IPTG) (final concentration: 1`mM) when OD_{600} = 0.7. After 7 h incubation at 37°C and 160 rpm, centrifugation was done at 5000 g, 4°C for 10 min. Cell pellet was suspended in Tris-EDTA buffer (Tris 1 M, EDTA 0.5 M) and sonicated three times for 45 s at 200 W, cycle 0.5 s with 1 min resting on ice in intervals for disruption of the cell wall. Lysate was centrifuged (17500 g, 4°C, 20 min) and the pellet was disolved in denaturing buffer (10 mM Tris-HCl, 100 mM H_2PO_4, 8 M urea, pH 8). The solution was centrifuged at 17500 g, 4°C for 20 min and supernatant was used for protein purification using Ni-NTA column. Nonspecific proteins were removed with wash buffer and the recombinant protein was collected from elutions based on imidazole concentration gradient. A sample from each fraction was mixed with SDS-loading buffer, boiled for 10 min. The analysis was carried out by sodium dodecyl sulfate polyacrylamide gel electrophoresis (SDS-PAGE) on 12% polyacrylamide gel. The

purified protein was dialyzed against 6 M urea, 4 M urea, 2 M urea, and phosphate buffered saline (PBS) (pH 7.2) at 4 °C for 2 h. Finally, the concentration of the proteins calculated by Bradford chromogenic assay.

Western blot analysis.
For western blotting, the separated protein by SDS-PAGE was transferred onto a nitrocellulose membrane. To avoid nonspecific reaction, blocking of the membrane was performed by 5% w/v skim milk in PBS containing 0.05% Tween 20 (PBST) at 4°C overnight. After three times washing the membrane with PBST, it was incubated with Horseradish peroxidase (HRP)-conjugated anti-His antibody (1:8000) at room temperature for 2 h. The membrane was washed three times and then diaminobenzidine (DAB) was added as a substrate of conjugated antibody. Finally, PBST was added to stop the reaction.

Cytotoxicity of recombinant proteins.
Cytotoxicity assay of the studied protein was performed using A549 cells (human lung epithelial cell line). Cells were cultured in 10% FBS supplemented DMEM, penicillin (1 mg/ml), and 50 mg/ml streptomycin at 37°C with 5% CO_2. 1×10^4 cell/well in 96-well tissue culture plates were incubated overnight under the aforementioned conditions. Solutions containing 0, 20, 40, and 80 µg/ml of the recombinant protein in the medium were prepared and added to each well. After incubation for 48 h, 20 µl 3-(4,5-dimethylthiazol-2- yl)-2-,5-diphenyltetrazolium bromide (MTT) (5 mg/ml) was added and incubated for additional 4 h at 37°C. The supernatant was then gently removed and 100 µl DMSO was added to solubilize formazan crystals. Finally, the absorbance was recorded at 570 nm.

Specific antibody production and measurement.
Female BALB/c mice of six to eight week age were purchased from Razi Vaccine and Serum Research Institute (Iran). The mice were placed in the animal house at the Shahed University under standard conditions. The research was conducted in compliance with the principles specified in the Guide for the Care and Use of laboratory animals. Ethical approval was issued by Shahed University. The animals were maintained in a well-ventilated environment with water and animal feed ad libitum. To induce specific antibody production, three doses of the recombinant protein (20 µg) mixed with Freund's adjuvant (1:1 (v/v)) were subcutaneously administered at final volume of 100 µl. Freund's Complete Adjuvant (FCA) was used for the first dose. Booster doses were administered 14 and 28 days after the first injection using Freund's Incomplete Adjuvant (FIA). Blood was collected from retro-orbital sinus on days 13th, 27th, and 41th. Sera were separated by centrifugation at 4000 g for 15 min and analyzed for antibody response. Specific IgG antibodies against the recombinant protein were analyzed by ELISA. A 96 well ELISA plate was coated with the protein in coating buffer (carbonate-bicarbonate, pH 9.6) in a final concentration of 5 µg/well at 4°C overnight. After blocking with 5% skim milk (w/v) in PBST at 37°C for 45 min, the wells were washed three times with PBST and serial dilution of sera were added followed by incubation at 37°C for 2 h. Each dilution was repeated for two times. The plates were washed three times and then Horseradish peroxidase-conjugated goat anti mouse IgG (diluted 1:15000) was added 100 µl/well and was incubated at 37°C for 1 h. The plates were washed and then 3,3′,5,5′-tetramethylbenzidine (TMB) substrate was added to each well at room temperature in darkness. After stopping the reaction with H_2SO_4 3M, the absorbance was recorded at 450 nm with ELISA reader.

Whole-cell ELISA test.
A. baumannii ATCC19606 was cultured in LB broth under iron limited condition. 100 µl of coating buffer containing 10^8 CFU of washed bacteria at logarithmic phase (OD_{600} = 0.6) was coated on 96-well plate at 4 °C overnight. The plate was dried and washed with PBST. The rest of the process is similar to ELISA. Specific antibody against the recombinant protein and HRP-conjugated anti-IgG were used as primary and secondary antibodies.

Bacterial challenge.
Since most of *A. baumannii* strains cause a self-limiting infections in common mouse models, the mixture of bacterial inoculum and mucin was used to establish a stable and lethal sepsis infection [38]. Bacterial cells were collected at mid-log phase. The bacterial suspension was mixed with 10% porcine mucin type II (w/v; Sigma-Aldrich). 500 µl of this mixture was injected to the mice intraperitoneally. Bacterial load was counted by plating a serial dilutions on LB agar. Lethal dose (LD_{100}) was determined by infecting mice with various concentrations of bacterial suspension ranging from 10^3 to 10^7 CFU/ml. The bacterial concentration leading to 100% mortality within 48 h was selected as LD_{100}. De-complemented sera from immunized mice obtained after the last booster dose, was prepared by incubation at 56°C for 30 min. Serum was administered intravenously 3 h prior to bacterial challenge. The mice were monitored for 7 days and survival number from each group was recorded every day.

Statistical analysis.
GraphPad Prism version 8.0.1 software was used for statistical analysis. Mean ± standard deviation (SD) was used to present the data. The data were analyzed by One-way ANOVA with Dunnett's multiple comparison test or *t*-test for a single comparison. $P \leq 0.05$ was considered significant.

3. RESULTS

Sequence frequency.
BLASTp of the sequence showed that 3472 strains of *A. baumannii* shared ≥99% query coverage, ≥ 97% identity (E-value 0) with the template. This protein is an outer membrane channel with TonB-dependent siderophore receptor domain.

Physicochemical characterization and protein localization.
First 44 amino acids were predicted as a signal peptide. The total number of amino acids were 728 with 80.5 kDa molecular weight. There is no cysteine residue in the protein sequence. Theoretically calculated pI was 5.61. As a result, the protein was acidic in nature. Total number of negatively and positively charged residues were 73 and 68 respectively. Instability index was computed 22.79 which indicated WP_000413999 is a stable protein in a test tube, as it was below cut-off value of 40. The aliphatic index was

calculated based on relative volume occupied by aliphatic amino acid side chain. This value for our protein was 72.40, which indicates thermostability of the protein over a wide temperature range. Protein's GRAVY value is sum of hydropathy values of all the amino acids per total number of amino acids in a sequence. This value was -0.474 for WP_000413999, showing its hydrophilic nature as well as its better interaction with water. Its estimated half-life was more than 10 h in *Escherichia coli*. According to BOMP analysis, the query protein was categorized at maximum level 5 as an integral outer membrane protein where level 1 is the least reliable prediction. In this regard, WP_000413999 was predicted as an outer membrane transporter by TMBETADISC-RBF. Furthermore, other servers demonstrated outer membrane localization of our protein with receptor activity in ion transportation.

Two and three dimensional structure and positioning in the membrane.

SEGMER predicted about 43.8% (319 amino acids) and 3.5% (26 amino acids) of the protein as β-strand and α-helix, respectively (Fig. 1).

Figure 1. Secondary structure prediction of WP_000413999. First line shows protein sequence and the next one depicts secondary structure prediction. E and H represent strand and helix, respectively.

PSI-blast introduced 5FP2_A, siderophore receptor Pira from *Pseudomonas aeruginosa*, as a structural template with query coverage 92%, E value 3e⁻139 and identity 18%. Tertiary structures modeled by servers together with their evaluations obtained from Qmean value and Ramachandran plot were listed in Table S1. Model No. 2 predicted by Robetta server presented the highest quality. Therefore, it was selected for further analysis. Values of z-score and also percentages of residues in favored, allowed, and outlier regions of the selected model were -2.38, 92.6%, 5.2%, and 2.2%, respectively. The higher the z-score of a model, the better the quality of the model. 3Drefine server presented 5 refined models for the query model served in PDB format. Structural validation of refined the selected model was carried out by the result obtained from Qmean server and Ramachandran plot. Some refined models presented improvement in Ramachandran plot criteria without significant changes in z-score. We selected the model as a final model with improved evaluation factors with emphasize on z-score relative to primary model. In the final model, Qmean z-score was -1.19. 92.8% of residues were present in the favored region while 5.2% of amino acids were presented in the allowed region and 1.9% residues were

present in disallowed regions of Ramachandran plot. The 3D structure of the final improved model was depicted in Figure 2a-b. The positioning of membrane protein in the bilayer outer membrane can help analyze surface exposed regions. PPM server predicted the orientation of WP_000413999 in the outer membrane. As shown in Figure 2 c-d some portions of β-sheets were above relative to membrane.
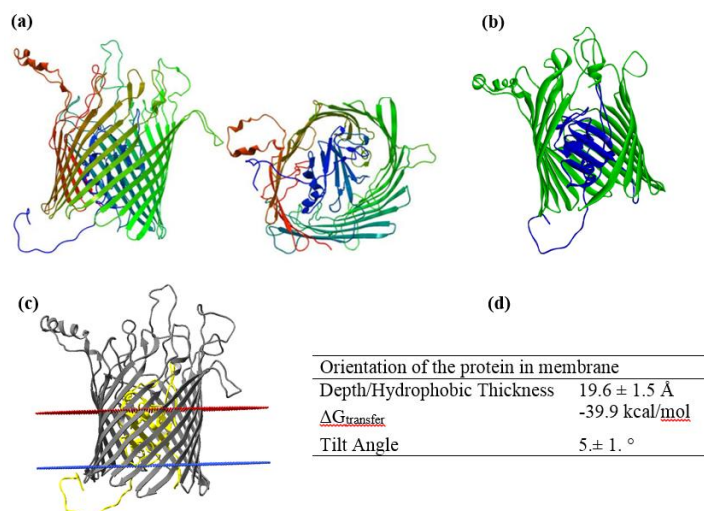
Figure 2. Tertiary structure and Orientation of WP_000413999 in the cell membrane. **(a)** 3D structure of refined final predicted model in rainbow color as N→C. **(b)** The plug domain (blue ribbons) position inside the barrel domain (green ribbons). **(c)** Membrane position of WP_000413999 predicted by PPM server, membrane bilayer surface depicted as red and blue dots, and the plug domain was shown by yellow ribbons. **(d)** Calculated orientation parameters by PPM, hydrophobic thickness for transmembrane proteins (A°), water to membrane transfer energy (ΔGtransfer, kcal/mol), and tilt angle (°), the angle between the peptide axis and the bilayer.

PCR amplification and Production of recombinant proteins.

The presence of gene encoding WP_000413999 was confirmed in standard and clinical strains by PCR. As expected, PCR led to amplification of a fragment about 2212 bp in length (Fig 3a).
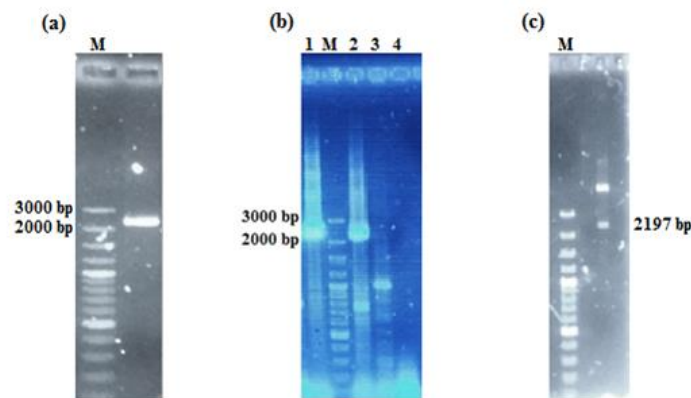
Figure 3. PCR amplification and cloning confirmation. **(a)** PCR product of gene encoding WP_000413999 using clinical isolate ABI022. **(b)** Cloning confirmation by PCR. Lane 1 and 2: positive clones, Lane 3: negative clone, Lane 4: negative control (without primers in PCR mixture). **(c)** Cloning confirmation by enzymatic digestion of positive clone. M: DNA ladder.

Clones containing recombinant vectors were confirmed by colony PCR using specific primers, digestion, and sequencing using universal primers (Fig. 3b-c). The recombinant protein was expressed as inclusion bodies in the host cell cytoplasm. Therefore, the protein was solubilized and purified under denaturing condition using buffers containing 8M urea (Fig. 4a).

Dialysis was used for the gradual removal of urea and then the recombinant protein was confirmed by western blot (Fig. 4b).
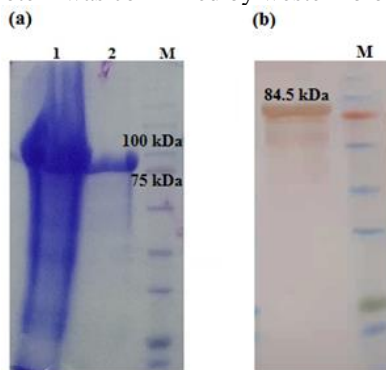
Figure 4. Production of recombinant protein. **(a)** SDS-PAGE of the protein, lane 1: induced WP_000413999, lane 2: purified WP_000413999. **(b)** Western blotting of the protein. M: Protein ladder.

In vitro toxicity assay of the recombinant protein.

For toxicity assay, the viability of A549 cells was analyzed in the presence of different concentrations of the studied protein. Survival rates of the cells were 99%, 96%, and 89% for 20, 40, and 80 µg/ml protein, respectively. There were no statistical differences between test and control groups ($p > 0.05$) (Fig. 5).
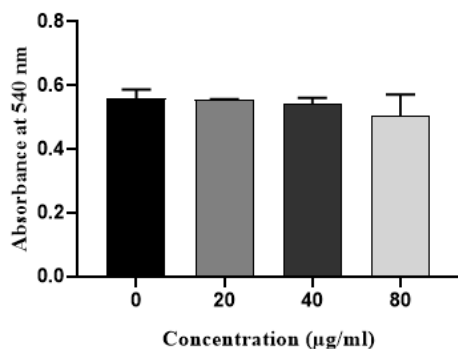
Figure 5. Cytotoxicity effect of the recombinant protein. MTT assay was performed on A549 cell line with different concentrations of the WP_000413999. **Antibody response.**

Indirect ELISA of sera from immunized and control mice indicated that specific IgG levels against each recombinant proteins were increased after the booster doses (Fig. 6a). Results of whole cell ELISA showed significant difference between immune and non-immune sera against intact *A. baumannii* ATCC 19606 (Fig. 6b).
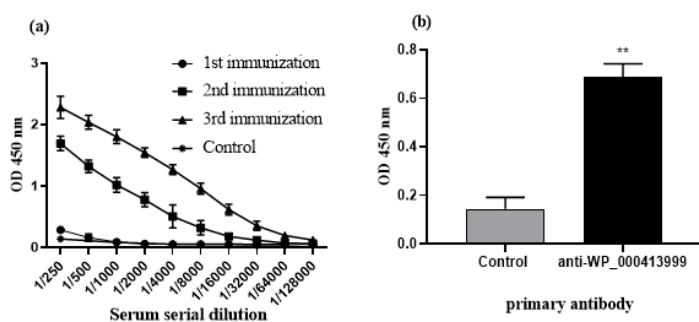
Figure 6. Indirect ELISA of immune and non-immune serum. **(a)** Total IgG levels of sera collected from mice after each immunization. **(b)** Interaction between anti-WP_000413999 and *A. baumannii* ATCC 19606 showed significant value ($p < 0.01$) as compared to control group. Serum was analyzed at 1:50 dilution. Serum from unimmunized mice was used for the control group.

Efficacy of antibody response.

1.5×10^6 CFU/ml and 5×10^4 CFU/ml were determined as *A. baumannii* ATCC 19606 and ABI022 lethal doses, respectively. These doses led to the death of the healthy unimmunized mice within 48 h in the murine model of sepsis. Therefore, ABI0022 was more virulent than ATCC 19606. Survival rates of the mice passively immunized with antisera against *A. baumannii* ATCC 19606 and ABI0022 challenges were measured 50 % and 40 %, respectively (Fig. 7).
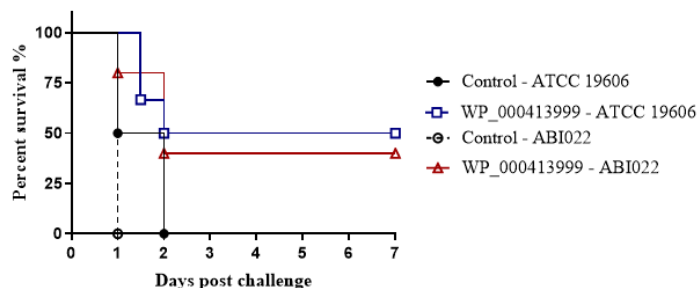
Figure 7. Survival rate of immunized mice. The mice were immunized intravenously with 100 µl of serum derived from actively immunized mice. Three hours later, the mice were intraperitoneally challenged with *A. baumannii* ATCC 19606 (n=6) or ABI022 (n=5) lethal dose.

Discussion.

Despite numerous studies devoted to *A. baumannii*, as a major threatening clinical factor, there are still quite a few unknown crucial aspects in developing new approaches to control the infections [1]. Using specific antibodies is considered as a strategy to prevent the *A. baumannii* infections for high risk persons [39, 40]. Iron uptake system, as an important virulence factor of *A. baumannii*, has been studied in terms of functionality, pathogenicity, and immunogenicity [11, 41-47]. WP_000413999, a siderophore receptor from cluster I, is strongly expressed in the early stages of bacteremia [26]. Moreover, Ni and collogues [48] reported this protein as a vaccine candidate using reverse vaccinology. In this study, we made an attempt to determine the physicochemical characteristics, 3D structure, and immunogenic properties of WP_000413999 followed by their evaluation in the experimental animal model.

Our *in silico* studies revealed that WP_000413999 classified as TonB dependent transporters (TBDTs) family expressed in outer membrane. This protein is a conserved thermo-stable hydrophilic molecule with high prevalence among strains of *A. baumannii*. These are attractive features of an immunogenic protein to be produced *in vitro* [4, 7]. Secondary structure of the protein is among the properties giving important insights into the correct and stable 3D structure of the proteins. Involvement of the majority of the amino acids involved with β-strands was demonstrated by secondary structure prediction. This result is consistent with β-barrel membrane nature of WP_000413999. Homology modeling is the best approach for determination of tertiary structure. However, the highest record in PSI-BLAST for choosing a template for our protein showed 18% structural similarity. Because the predicted models by homology modelling under 30% similarity are not reliable [49], we applied other methods to predict 3D-structure of WP_00041399. Amongst various servers, Robetta server based on ab initio modelling offered the best model with higher Qmean z-score. In this model, WP_000413999

contains plug and β-barrel domains. The first 150 residues after signal peptide, at the N-terminus formed the plug domain placed in β-barrel lumen, acts as a barrier for small molecules entering the cell [50]. The barrel is composed of 22 antiparallel transmembrane β-strands expanded in the lipid bilayer. The strands are connected with external loops and periplasmic turns (Fig. 2). In the barrel domain, 39% and 55% of amino acids contributed to membrane region and exposed loops, respectively. As a result, WP_000413999 is a partially exposed protein which can interact with specific antibodies by its extracellular loops. In a study conducted by Esmaeilkhani et al., the raised antibodies against BauA, as an outer membrane receptor of iron uptake system could control *A. baumannii* infection [11]. Based on *in vitro* study of Goel et al., this protection was probably provided because of the receptor dysfunction as well as opsonophagocytic effect of antibodies [45].

Our recombinant protein showed no significant toxicity with ability to induce an antibody response. Specific antibody levels increased after the booster doses which indicates immunogenicity of studied protein. These antibodies are capable of interacting with native protein on the surface of the experimental strain (Fig. 6b). Therefore, it was predicted that antibodies against studied protein would protect the infected animal model. In this study, partial protection against *A. baumannii* lethal dose was achieved in passively immunized mice. Antisera against single recombinant proteins in the previous studies induced relative to complete protection [7-9, 15, 40]. In the current study, the survival rate was higher against *A. baumannii* ATCC 19606 compared to clinical isolate, ABI022. It may be due to the different expression pattern of WP_000413999 on the bacterial surface. On the other hand, exposure of OMPs can be affected by capsule thickness [51]. However, studies continue on the surface bacterial structures as potential vaccine targets [40, 52, 53]. Therefore, further investigations are required to ensure the suggested reasons. Evaluation of specific avian antibodies (IgY) against OmpA, Omp34, and inactivated the whole cell in a pneumonia model showed that IgY-OmpA yielded the highest prophylactic effect [40] which is inconsistent with the results by Wang et al. [51]. This contradiction can be due to a different type of capsule in studied clinical isolates. In another study, passive immunization with anti-Ata decreased the bacterial count in the lungs of challenged mice. Even though its expression level is variable among *A. baumannii* strains, this protein is considered as a valuable vaccine candidate because of its high conservancy and importance in bacterial virulence [5, 54].

4. CONCLUSIONS

In conclusion, specific antibodies against recombinant WP_000413999, a siderophore receptor from *A. baumannii*, could interact with native protein on the surface of pathogen. They also increase the survival rate of mice passively immunized compared to control group in the murine sepsis model. Our results demonstrated that WP_000413999 is a conserved non-toxic immunogen. So, this antigen could be considered as a component of multivalent vaccine formulation in active and passive immunization strategies.

5. REFERENCES

1. Wong, D.; Nielsen, T. B.; Bonomo, R. A.; Pantapalangkoor, P.; Luna, B.; Spellberg, B. Clinical and pathophysiological overview of *Acinetobacter* infections: a century of challenges. *Clinical microbiology reviews* **2017**, *30*, 409-447, http://dx.doi.org/10.1128/CMR.00058-16.

2. Harding, C.M.; Hennon, S.W.; Feldman, M.F. Uncovering the mechanisms of *Acinetobacter baumannii* virulence. *Nature Reviews Microbiology* **2018**, *16*, 91-102, https://doi.org/10.1038/nrmicro.2017.148.

3. Tacconelli, E,; Magrini, N.; Kahlmeter, G.; Singh, N . Global priority list of antibiotic-resistant bacteria to guide research, discovery, and development of new antibiotics. *World Health Organization* **2017**, https://www.who.int/medicines/publications/WHO-PPL-Short_Summary_25Feb-ET_NM_WHO.pdf

4. Luo, G.; Lin, L.; Ibrahim, A.S.; Baquir, B.; Pantapalangkoor, P.; Bonomo, R.A.; Doi, Y.; Adams, M.D.; Russo, T.A.; Spellberg, B. Active and passive immunization protects against lethal, extreme drug resistant-*Acinetobacter baumannii* infection. *PloS one* **2012**, *7*, 29446, https://doi.org/10.1371/journal.pone.0029446.

5. Bentancor, L.V.; Routray, A.; Bozkurt-Guzel, C.; Camacho-Peiro, A.; Pier, G.B.; Maira-Litrán, T. Evaluation of the trimeric autotransporter Ata as a vaccine candidate against *Acinetobacter baumannii* infections. *Infection and Immunity* **2012**, *80*, 3381-3388, https://doi.org/10.1128/IAI.06096-11.

6. Fattahian, Y.; Rasooli, I.; Mousavi, G.S..L.; Rahbar, M.R.; Darvish, A.A.S.; Amani, J. Protection against *Acinetobacter baumannii* infection via its functional deprivation of biofilm associated protein (Bap). *Microbial Pathogenesis* **2011**, *51*, 402-406, https://doi.org/10.1016/j.micpath.2011.09.004.

7. Huang, W.; Yao, Y.; Wang, S.; Xia, Y.; Yang, X.; Long, Q.; Sun, W.; Liu, C.; Li, Y.; Chu, X. Immunization with a 22-kDa outer membrane protein elicits protective immunity to multidrug-resistant *Acinetobacter baumannii*. *Scientific Reports* **2016**, *6*, 20724, https://doi.org/10.1038/srep20724.

8. Huang, W.; Wang, S.; Yao, Y.; Xia, Y.; Yang, X.; Long, Q.; Sun, W.; Liu, C.; Li, Y.; Ma, Y. OmpW is a potential target for eliciting protective immunity against *Acinetobacter baumannii* infections. *Vaccine* **2015**, *33*, 4479-4485, https://doi.org/10.1016/j.vaccine.2015.07.031.

9. Garg, N.; Singh, R.; Shukla, G.; Capalash, N.; Sharma, P. Immunoprotective potential of in silico predicted *Acinetobacter baumannii* outer membrane nuclease, NucAb. *International Journal of Medical Microbiology* **2016**, *306*, 1-9, https://doi.org/10.1016/j.ijmm.2015.10.005.

10. Singh, R.; Garg, N.; Shukla, G.; Capalash, N.; Sharma, P. Immunoprotective efficacy of *Acinetobacter baumannii* outer membrane protein, FilF, predicted in silico as a potential vaccine candidate. *Frontiers in Microbiology* **2016**, *7*, 158, https://doi.org/10.3389/fmicb.2016.00158.

11. Esmaeilkhani, H.; Rasooli, I.; Nazarian, S.; Sefid, F. In vivo validation of the immunogenicity of recombinant baumannii acinetobactin utilization a protein (rBauA). *Microbial Pathogenesis* **2016**, *98*, 77-81, https://doi.org/10.1016/j.micpath.2016.06.032.

12. Yang, F.L.; Lou, T.C.; Kuo, S.C.; Wu, W.L.; Chern, J.; Lee, Y.T.; Chen, S.T.; Zou, W.; Lin, N.T.; Wu, S.H. A medically

relevant capsular polysaccharide in *Acinetobacter baumannii* is a potential vaccine candidate. *Vaccine* **2017**, *35*, 1440-1447, https://doi.org/10.1016/j.vaccine.2017.01.060.

13. Huang, W.; Yao, Y.; Long, Q.; Yang, X.; Sun, W.; Liu, C.; Jin, X.; Chu, X.; Chen, B.; Ma, Y. Immunization against multidrug-resistant *Acinetobacter baumannii* effectively protects mice in both pneumonia and sepsis models. *PloS one* **2014**, *9*, 100727, https://doi.org/10.1371/journal.pone.0100727

14. McConnell, M.J.; Pachón, J. Active and passive immunization against *Acinetobacter baumannii* using an inactivated whole cell vaccine. *Vaccine* **2010**, *29*, 1-5, https://doi.org/10.1016/j.vaccine.2010.10.052.

15. Singh, R.; Capalash, N.; Sharma, P. Immunoprotective potential of BamA, the outer membrane protein assembly factor, against MDR *Acinetobacter baumannii*. *Scientific Reports* **2017**, *7*, 12411, https://doi.org/10.1038/s41598-017-12789-3.

16. Pulido, M. R.; García-Quintanilla, M.; Pachón, J.; McConnell, M. J. Immunization with lipopolysaccharide-free outer membrane complexes protects against *Acinetobacter baumannii* infection. *Vaccine* **2018**, *36*, 4153-4156, http://doi.org/10.1016/j.vaccine.2018.05.113.

17. Li, H.; Tan, H.; Hu, Y.; Pan, P.; Su, X.; Hu, C. Small protein A and phospholipase D immunization serves a protective role in a mouse pneumonia model of *Acinetobacter baumannii* infection. *Molecular Medicine Reports* **2017**, *16*, 1071-1078, http://doi.org/10.3892/mmr.2017.6688.

18. Ainsworth, S.; Ketter, P. M.; Yu, J.-J.; Grimm, R. C.; May, H. C.; Cap, A. P.; Chambers, J. P.; Guentzel, M. N.; Arulanandam, B. P. Vaccination with a live attenuated *Acinetobacter baumannii* deficient in thioredoxin provides protection against systemic *Acinetobacter* infection. *Vaccine* **2017**, *35*, 3387-3394, http://doi.org/10.1016/j.vaccine.2017.05.017. 19. Gaddy, J.A.; Arivett, B.A.; McConnell, M.J.; López-Rojas, R.; Pachón, J.; Actis, L.A. Role of acinetobactin-mediated iron acquisition functions in the interaction of *Acinetobacter baumannii* strain ATCC 19606T with human lung epithelial cells, Galleria mellonella caterpillars, and mice. *Infection and Immunity* **2012**, *80*, 1015-1024, https://doi.org/10.1128/IAI.06279-11.

20. Liu, C.; Chang, Y.; Xu, Y.; Luo, Y.; Wu, L.; Mei, Z.; Li, S.; Wang, R.; Jia, X. Distribution of virulence-associated genes and antimicrobial susceptibility in clinical *Acinetobacter baumannii* isolates. *Oncotarget* **2018**, *9*, 21663-21673, https://doi.org/10.18632/oncotarget.24651. 21. Eijkelkamp, B.A.; Hassan, K.A.; Paulsen, I.T.; Brown, M.H. Investigation of the human pathogen *Acinetobacter baumannii* under iron limiting conditions. *BMC genomics* **2011**, *12*, 126, https://doi.org/10.1186/1471-2164-12-126.

22. Antunes, L.C.; Imperi, F.; Towner, K.J.; Visca, P. Genome-assisted identification of putative iron-utilization genes in *Acinetobacter baumannii* and their distribution among a genotypically diverse collection of clinical isolates. *Research in Microbiology* **2011**, *162*, 279-284, https://doi.org/10.1016/j.resmic.2010.10.010.

23. McConnell, M.J.; Domínguez-Herrera, J.; Smani, Y.; López-Rojas, R.; Docobo-Pérez, F.; Pachón, J. Vaccination with outer membrane complexes elicits rapid protective immunity to multidrug-resistant *Acinetobacter baumannii*. *Infection and Immunity* **2011**, *79*, 518-526, https://doi.org/10.1128/IAI.00741-10.

24. Nwugo, C.C.; Gaddy, J.A.; Zimbler, D.L.; Actis, L.A. Deciphering the iron response in *Acinetobacter baumannii*: a proteomics approach. *Journal of Proteomics* **2011**, *74*, 44-58, https://doi.org/10.1016/j.jprot.2010.07.010.

25. Kentache, T.; Abdelkrim, A.B.; Jouenne, T.; Dé, E.; Hardouin, J. Global dynamic proteome study of a pellicle-forming *Acinetobacter baumannii* strain. *Molecular & Cellular Proteomics* **2017**, *16*, 100-112, https://doi.org/10.1074/mcp.M116.061044.

26. Murray, G.L.; Tsyganov, K.; Kostoulias, X.P.; Bulach, D.M.; Powell, D.; Creek, D.J.; Boyce, J.D.; Paulsen, I.T.; Peleg, A.Y. Global gene expression profile of *Acinetobacter baumannii* during bacteremia. *The Journal of Infectious Diseases* **2017**, *215*, 52-57, https://doi.org/10.1093/infdis/jiw529.

27. Gasteiger, E.; Hoogland, C.; Gattiker, A.; Duvaud, S.E.; Wilkins, M.R.; Appel, R.D.; Bairoch, A. Protein identification and analysis tools on the ExPASy server. *Springer:* **2005**, https://doi.org/10.1385/1-59259-890-0:571.

28. Berven, F.S.; Flikka, K.; Jensen, H.B.; Eidhammer, I. BOMP: a program to predict integral β-barrel outer membrane proteins encoded within genomes of Gram-negative bacteria. *Nucleic Acids Research* **2004,** *32*, 394-399, https://doi.org/10.1093/nar/gkh351.

29. Ou, Y.Y.; Gromiha, M.M.; Chen, S.A.; Suwa, M. TMBETADISC-RBF: Discrimination of β-barrel membrane proteins using RBF networks and PSSM profiles. *Computational Biology and Chemistry* **2008**, *32*, 227-231, https://doi.org/10.1016/j.compbiolchem.2008.03.002.

30. Yu, C.S.; Cheng, C.W.; Su, W.C.; Chang, K.C.; Huang, S.W.; Hwang, J.K.; Lu, C.H. CELLO2GO: a web server for protein subCELlular LOcalization prediction with functional gene ontology annotation. *PLoS One* **2014**, *9*, 99368, https://doi.org/10.1371/journal.pone.0099368.

31. Wu, S.; Zhang, Y. Recognizing protein substructure similarity using segmental threading. *Structure* **2010**, *18*, 858-867, https://doi.org/10.1016/j.str.2010.04.007.

32. Yang, J.; Zhang, Y. Protein Structure and Function Prediction Using I-TASSER. *Current protocols in bioinformatics* **2015**, *52*, 5.8.1-5.8.15, https://doi.org/10.1002/0471250953.bi0508s52.

33. Yang, Y.; Faraggi, E.; Zhao, H.; Zhou, Y. Improving protein fold recognition and template-based modeling by employing probabilistic-based matching between predicted one-dimensional structural properties of query and corresponding native properties of templates. *Bioinformatics* **2011**, *27*, 2076-2082, https://doi.org/10.1093/bioinformatics/btr350.

34. Kim, D.E.; Chivian, D.; Baker, D. Protein structure prediction and analysis using the Robetta server. *Nucleic Acids Research* **2004**, *32*, 526-531, https://doi.org/10.1093/nar/gkh468.

35. Benkert, P.; Tosatto, S.C.; Schomburg, D. QMEAN: A comprehensive scoring function for model quality assessment. *Proteins* **2008**, *71*, 261-277, https://doi.org/10.1002/prot.21715.

36. Bhattacharya, D.; Cheng, J. 3Drefine: Consistent protein structure refinement by optimizing hydrogen bonding network and atomic-level energy minimization. *Proteins* **2013**, *81*, 119-131, https://doi.org/10.1002/prot.24167.

37. Lomize, M.A.; Pogozheva, I.D.; Joo, H.; Mosberg, H.I.; Lomize, A.L. OPM database and PPM web server: resources for positioning of proteins in membranes. *Nucleic Acids Research* **2012**, *40*, 370-376, https://doi.org/10.1093/nar/gkr703.

38. Harris, G.; KuoLee, R.; Xu, H. H.; Chen, W. Mouse Models of *Acinetobacter baumannii* Infection. *Current Protocols in Microbiology* **2017**, *46*, 6G. 3.1-6G. 3.23, http://dx.doi.org/10.1002/cpmc.36.

39. Pachón, J.; McConnell, M.J. Considerations for the development of a prophylactic vaccine for *Acinetobacter baumannii*. *Vaccine* **2014**, *32,* 2534-2536, https://doi.org/10.1016/j.vaccine.2013.10.064.

40. Jahangiri, A.; Owlia, P.; Rasooli, I.; Salimian, J.; Derakhshanifar, E.; Naghipour Erami, A.; Darzi Eslam, E.; Darvish Alipour Astaneh, S. Specific egg yolk antibodies (IgY) confer protection against *Acinetobacter baumannii* in a murine pneumonia model. *Journal of Applied Microbiology* **2018,** *126*, 624-632, https://doi.org/10.1111/jam.14135.

41. Runci, F.; Gentile, V.; Frangipani, E.; Rampioni, G.; Leoni, L.; Lucidi, M.; Visaggio, D.; Harris, G.; Chen, W.; Stahl, J.; Averhoff, B.; Visca, P. Contribution of Active Iron Uptake to *Acinetobacter baumannii* Pathogenicity. *Infection and Immunity* **2019**, *87*, e00755-00718, http://doi.org/10.1128/IAI.00755-18.

42. Álvarez-Fraga, L.; Vázquez-Ucha, J. C.; Martínez-Guitián, M.; Vallejo, J. A.; Bou, G.; Beceiro, A.; Poza, M. Pneumonia infection in mice reveals the involvement of the feoA gene in the pathogenesis of *Acinetobacter baumannii*. *Virulence* **2018**, *9*, 496-509, http://doi.org/10.1080/21505594.2017.1420451.

43. Sangroodi, Y.H.; Rasooli, I.; Nazarian, S.; Ebrahimzadeh, W.; Sefid, F. Immunogenicity of conserved cork and β-barrel domains of Baumannii Acintobactin Utilization protein in animal model. *Turkish journal of medical sciences* **2015**, *45*, 1396-1402, https://doi.org/10.3906/sag-1407-45.

44. Sefid, F.; Rasooli, I.; Jahangiri, A.; Bazmara, H. Functional Exposed Amino Acids of BauA as Potential Immunogen Against *Acinetobacter baumannii*. *Acta Biotheoretica* **2015**, *63*, 129-149, https://doi.org/10.1007/s10441-015-9251-2.

45. Goel, V.K.; Kapil, A. Monoclonal antibodies against the iron regulated outer membrane proteins of *Acinetobacter baumannii* are bactericidal. *BMC microbiology* **2001**, *1*, 16, https://doi.org/10.1186/1471-2180-1-16.

46. Zimbler, D.L.; Penwell, W.F.; Gaddy, J.A.; Menke, S.M.; Tomaras, A.P.; Connerly, P.L.; Actis, L.A. Iron acquisition functions expressed by the human pathogen *Acinetobacter baumannii*. *Biometals* **2009**, *22*, 23-32, https://doi.org/10.1007/s10534-008-9202-3.

47. Mihara, K.; Tanabe, T.; Yamakawa, Y.; Funahashi, T.; Nakao, H.; Narimatsu, S.; Yamamoto, S. Identification and transcriptional organization of a gene cluster involved in biosynthesis and transport of acinetobactin, a siderophore produced by *Acinetobacter baumannii* ATCC 19606T. *Microbiology* **2004**, 150, 2587-2597, https://doi.org/10.1099/mic.0.27141-0.

48. Ni, Z.; Chen, Y.; Ong, E.; He, Y. Antibiotic resistance determinant-focused *Acinetobacter baumannii* vaccine designed using reverse vaccinology. *International Journal of Molecular Sciences* **2017**, *18*, *458*, https://doi.org/10.3390/ijms18020458.

49. Rigden, D.J.; From protein structure to function with bioinformatics. *Springer* **2017**, https://doi.org/10.1007/978-94-024-1069-3.

50. Noinaj, N.; Guillier, M.; Barnard, T.J.; Buchanan, S.K. TonB-dependent transporters: regulation, structure, and function. *Annual Review of Microbiology* **2010**, *64*, 43-60, https://doi.org/10.1146/annurev.micro.112408.134247.

51. Wang-Lin, S.X.; Olson, R.; Beanan, J.M.; MacDonald, U.; Balthasar, J.P.; Russo, T.A. The capsular polysaccharide of *Acinetobacter baumannii* is an obstacle for therapeutic passive immunization strategies. *Infection and immunity* **2017**, https://doi.org/10.1128/IAI.00591-17.

52. Song, X.; Zhang, H.; Zhang, D.; Xie, W.; Zhao, G. Bioinformatics analysis and epitope screening of a potential vaccine antigen TolB from *Acinetobacter baumannii* outer membrane protein. *Infection, Genetics and Evolution* **2018**, *62*, 73-79, https://doi.org/10.1016/j.meegid.2018.04.019.

53. Guo, S. J.; Ren, S.; Xie, Y. E. Evaluation of the Protective Efficacy of a Fused OmpK/Omp22 Protein Vaccine Candidate against *Acinetobacter baumannii* Infection in Mice. *Biomedical and Environmental Sciences* **2018**, *31*, 155-158, https://doi.org/10.3967/bes2018.019.

54. Weidensdorfer, M.; Ishikawa, M.; Hori, K.; Linke, D.; Djahanschiri, B.; Iruegas, R.; Ebersberger, I.; Riedel-Christ, S.; Enders, G.; Leukert, L.; Kraiczy, P.; Rothweiler, F.; Cinatl, J.; Berger, J.; Hipp, K.; Kempf, V. A. J.; Göttig, S. The Acinetobacter trimeric autotransporter adhesin Ata controls key virulence traits of Acinetobacter baumannii. *Virulence* **2019**, *10*, 68-81, http://dx.doi.org/10.1080/21505594.2018.1558693.

6. ACKNOWLEDGEMENTS

Table S1. Predicted tertiary structures by diverse methods and their evaluations. Higher amount of z-score, and amino acids in favored and allowed regions are desired.

Server	Model	Qmean z-score	Ramachandran plot		
			favoured region	allowed region	outlier region
I-TASSER	model 1	-20.15	50.6	26.3	23.1
I-TASSER	model 2	-18.14	61.3	19.8	18.9
I-TASSER	model 3	-16.4	60.2	19	20.8
I-TASSER	model 4	-13.97	67.1	19.4	13.5
sparks-x	model 1	-7.08	90.5	6.6	2.9
sparks-x	model 2	-7.51	89.4	8	2.6
sparks-x	model 3	-8.11	89.3	6.3	4.4
sparks-x	model 4	-8.03	89.9	6.6	3.4
sparks-x	model 5	-7.09	90.8	6.3	2.9
sparks-x	model 6	-8.49	89.7	6.5	3.9
sparks-x	model 7	-7.77	89.9	6.1	4
sparks-x	model 8	-6.87	91.7	5.6	2.6
sparks-x	model 9	-8.36	89.7	6.3	4
sparks-x	model 10	-8.3	90.9	5.6	3.4
Robetta	model 1	-3.27	88.6	9.4	2.1
Robetta	**model 2**	**-2.38**	**92.6**	**5.2**	**2.2**
Robetta	model 3	-3.39	87.9	9	3.2
Robetta	model 4	-2.93	89.3	7.9	2.9
Robetta	model 5	-4.29	86.2	9.9	3.9

The box represents the selected model.